Optimal Spacecraft Tracking under Limited Signal Level and High Trajectory Dynamics

Timothy T. Pham

Jet Propulsion Laboratory
California Institute of Technology
4800 Oak Grove Drive
Pasadena, California 91109, USA
Email: Timothy.Pham@jpl.nasa.gov

In deep space communications, signal power is often limited due to the vast interplanetary distance. Accordingly, the receiver tracking bandwidth needs to be as narrow as possible to maximize signal detection. Yet, there are periods in mission operations such as during a planetary encounter that the trajectory is subject to large dynamic uncertainty. This condition, in turn, requires a wider bandwidth setting in order to maintain receiver lock. An optimal bandwidth is the one that satisfies these two constraints and thus, minimizes the data outage.

This paper illustrates such a consideration by analyzing several encounters that the Galileo spacecraft has made with Jupiter's moons. The foundation for this analysis is presented. Results from actual encounters are compared against predictions. Operational strategies that can be taken to mitigate the impact are identified.

I. INTRODUCTION

In deep space communications, signal power is usually of premium value. Due to the expensive launch cost, spacecraft is often equipped with limited transmitting power and small antenna. The vast interplanetary distance drastically reduces the received signal power following the inverse law of the distance squared. The limited received signal power makes spacecraft tracking a challenge, in particular for those exploring the outer planetary region of the solar system. It is desirable to operate the receiver with the smallest tracking bandwidth possible. Such a setting allows for maximum signal detection and minimum processing loss.

However, there are several opposing forces that preclude the use of small bandwidth. Phase noise inherent in the signal is one factor. The phase noise is caused by the frequency instability of the spacecraft oscillators or by the intervening propagation medium. This noise effectively smears the signal carrier, changing it from an ideal single-frequency tone to a signal that occupies some finite bandwidth. In order to capture all signal energy, the receiver bandwidth has to be widened. The uncertainty in spacecraft trajectory at the time of close encounter with planetary bodies is another factor that requires wider tracking bandwidth. The trajectory error is translated to a frequency error. The frequency error then dictates a need for wider bandwidth in order to maintain receiver lock.

An optimal bandwidth, obviously, is the one that satisfies the constraints imposed by low signal-to-noise ratio (SNR) and high dynamics. In the best scenarios, both constraints are met. When they are not, some tradeoffs are needed. The Galileo mission offers a good case for study of optimal bandwidth setting. Launched in October 1989, the spacecraft embarked on a 6-year journey on route to Jupiter. Its trajectory included a flyby with Venus and two Earth flybys to gain the necessary gravity assisted momentum for its destination. Once reaching Jupiter in 1995, the Galileo spacecraft has made several encounters with Jupiter and the Jovian satellites. Important scientific observations were made each time the spacecraft closely approached the four major moons of Jupiter - Io, Europa, Ganymede and Callisto. Figure 1 presents the trajectory of Galileo during its prime and extended missions [1].

In what follows, Section II will provide a brief review on the analytical foundation. Section III will show the data analysis and comparison between expected and actual performance on selected encounters that Galileo has made with the Jovian satellites. Some strategies that were taken, or could have been taken, to ensure successful tracking will be identified.
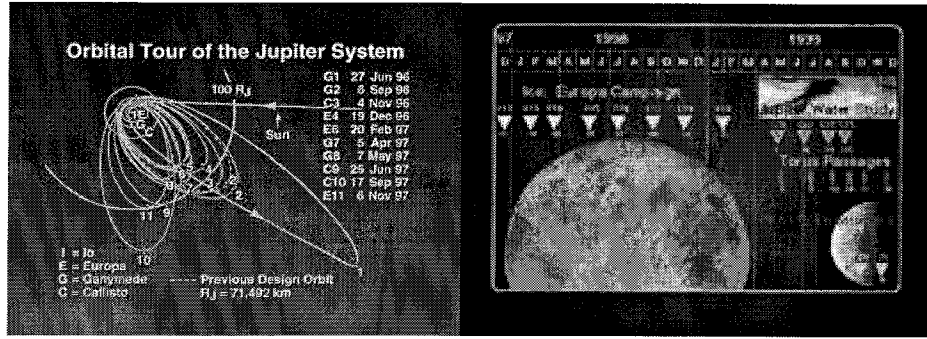
Fig. 1: Encounters with Jovian satellites during Galileo prime and extended missions

II. ANALYTICAL FOUNDATION

In this section, we will review the basic operation of phase lock loop (PLL), which is at the heart of receiver tracking functions. A more thorough treatment of this topic can be found in [2]. We will examine the loop response to an input error. Both frequency rate and frequency acceleration errors are considered. From the thermal noise analysis viewpoint, we will also review the necessary bandwidth required to ensure proper tracking. An optimal bandwidth is the one that best satisfies the Doppler and thermal constraints. Since Galileo tracking support is done with two different receivers - one employs the second-order PLL, the other the third-order - the behavior difference between these two loops will be addressed. Aside from the steady state error, a consideration on transient error will also be given.

1. Basic operations of phase lock loop

Figure 2(a) shows the basic components of a phase lock loop. The three main components of the PLL are: a phase detector, a loop filter and a voltage controlled oscillator (VCO). The phase detector monitors how well tracking is taking place. The loop filter reduces the noisy error signal to a detected, stable signal that can be used for control purposes. The voltage control oscillator then corrects the phase error.
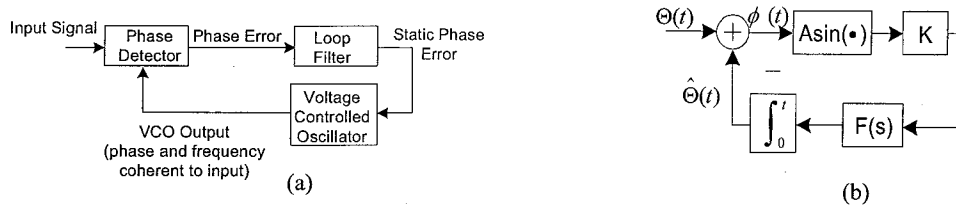

Fig. 2. (a) Basic components of PLL; (b) Baseband model

Figure 2(b) provides a mathematical representation of the PLL operation. The phase of the incoming signal, $\Theta(t)$, is tracked by its estimated counterpart, $\hat{\Theta}(t)$. The phase detector produces an error signal $\phi(t)$ that is proportional to the phase difference between its two inputs. The AK factor represents the loop gain, which includes the signal amplitude, the gain factors of the phase detector, loop filter and voltage control oscillator. A high loop gain, without causing an instability, is desirable since it increases the sensitivity of the loop response and suppresses the noise effect. The error signal is low-pass filtered by the loop filter F(s) so that minimal noise is present in the phase estimation. Second order loop filter is most often used due to its inherent stability. The filtered error signal is then used to drive the voltage control oscillator. The larger the error, the more frequency shift will occur at the VCO output to match up with the input. Since frequency is the derivative of phase with respect to time, an integral is used to model the VCO operation.

2. Doppler dynamic consideration

As Galileo approaches Jupiter's moons, its velocity and acceleration are affected by the moon's gravitation pull. This results in a change in the observed Doppler, as well as its derivatives. The perturbation is time varying with respect to

the spacecraft altitude as well as the geometry of Earth, spacecraft and the Jupiter's moon. The effect on the Doppler is typically in the order of kHz, and on the Doppler rate a few Hz. The effect generally lasts over 45 minutes. Much of this effect can be modeled and removed with the frequency-aided predictions. The uncertainty in the model however represents the remaining error in the input. Typically, the 1-sigma error constitutes about 1% - 5% of the whole effect. A sample profile of the Doppler profile for the Galileo encounter with Callisto (C3) is provided in Figure 3 [3].
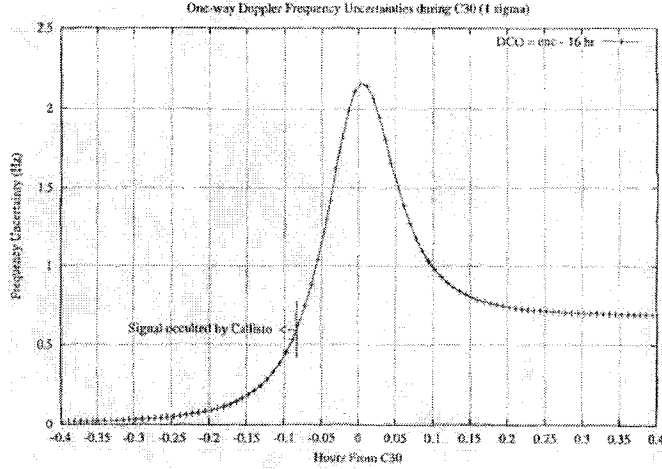

Fig. 3: Expected Doppler uncertainty for the C3 encounter

The received signal frequency can be modeled as:

$$f(t) = f_o + \Delta f + \frac{df}{dt} t + \frac{d^2 f}{dt^2} t^2$$

where f_o is the transmitted frequency without perturbation,

Δf is the perturbed Doppler error, in Hz,

$\dfrac{df}{dt}$ is the perturbed Doppler rate error, in Hz/s, and

$\dfrac{d^2 f}{dt^2}$ is the perturbed Doppler acceleration error, in Hz/s^2

The transmitted frequency f_o , including nominal Doppler effect, is not a problem since its values are well modeled. Only the un-modeled errors Δf , $\dfrac{df}{dt}$ and $\dfrac{d^2 f}{dt^2}$ need to be considered. The Laplace transform of these errors are:

Doppler offset: $\dfrac{\Delta f}{s^2}$

Doppler rate error: $\dfrac{df}{dt} \dfrac{1}{s^3}$

Doppler acceleration error: $\dfrac{d^2 f}{dt^2} \dfrac{1}{s^4}$

The phase change at the input can be represented as:

$$\Theta(s) = 2\pi \left(\frac{\Delta f}{s^2} + \frac{df}{dt} \frac{1}{s^3} + \frac{d^2 f}{dt^2} \frac{1}{s^4} \right) \tag{1}$$

The tracking performance of a phase lock loop is judged by the amount of phase error $\phi(t)$ remaining in the loop. The error, in turn, is dependent on the order of the loop filter. In most operating conditions, a second order loop offers sufficiently good performance. The third order loop, however, can remove the effect of high order dynamics and thus enable better tracking under a more dynamic condition. The drawback with the third order loop is a potential problem with the instability and the difficulty in signal acquisition.

The phase error, as a result of a change in the input, is [2, 4, 5]:

$$\Phi(s) = [1 - H(s)]\Theta(s) \tag{2}$$

where H(s) is the closed-loop transfer function and $H(s) = \dfrac{AKF(s)}{s + AKF(s)}$

For second order loop, $F_2(s) = \dfrac{1 + \tau_2 s}{\tau_1 s}$ where τ_i are the loop time constants.

For third order loop, $F_3(s) = \dfrac{1 + \tau_2 s}{\tau_1 s} + \dfrac{1}{\tau_1 \tau_3 s^2}$

Replacing appropriate F(s) function into (2), the phase error for 2nd and 3rd loop becomes:

$$\Phi_2(s) = \frac{\tau_1 s^2}{\tau_1 s^2 + AK\tau_2 s + AK} \Theta(s)$$

$$\Phi_3(s) = \frac{\tau_1 \tau_3 s^3}{\tau_1 \tau_3 s^3 + AK\tau_2\tau_3 s^2 + AK\tau_3 s + AK} \Theta(s)$$

With the aid of the final theorem of Laplace transform, (2a) and (2b), we can determine the steady state phase error.

$$\phi_{ss} = \lim_{t \to \infty} \phi(t) = \lim_{s \to 0} s\Phi(s)$$

$$\phi_{ss,2} = \lim_{s \to 0} \left[\frac{\tau_1 s^3}{\tau_1 s^2 + AK\tau_2 s + AK} \Theta(s) \right] \tag{2a}$$

$$\phi_{ss,3} = \lim_{s \to 0} \left[\frac{\tau_1 \tau_3 s^4}{\tau_1 \tau_3 s^3 + AK\tau_2\tau_3 s^2 + AK\tau_3 s + AK} \Theta(s) \right] \tag{2b}$$

Note that ϕ_{ss} is a product of a high order polynomial and the incoming input $\Theta(s)$. For second order loop, the polynomial is of order $O(s^3)$. The second order loop therefore can tolerate an input change in $\Theta(s)$ up to the order of $O(\dfrac{1}{s^3})$. Refer back to (1), we can see that the second order loop can handle a Doppler offset and Doppler rate error, but not the frequency acceleration. For third order loop, $\phi_{ss,3}$ contains a polynomial of order $O(s^4)$. It therefore can effectively track out the Doppler acceleration.

Combining (1), (2a), (2b), we can compute the steady state phase error. Expressed in term of loop bandwidth B_L, the steady state phase errors for the second and third order loop are identified in [6] as:

$$\varphi_{ss,2} = 2\pi \frac{1}{r} \left(\frac{r+1}{4B_{L,2}} \right)^2 \left(\frac{df}{dt} + \int_o^T \frac{d^2 f}{dt^2} dt \right) \text{ where } r = \frac{AK\tau_2^2}{\tau_1} \text{ and } B_{L,2} \cong \frac{r+1}{4\tau_2}$$

$$\varphi_{ss,3} = 2\pi \frac{1}{rk}\left(\frac{r}{4B_{L,3}}\left(\frac{r-k+1}{r-k}\right)\right)^3 \frac{d^2f}{dt^2} \quad \text{where } r = \frac{AK\tau_2^2}{\tau_1}; \ k = \frac{\tau_2}{\tau_3} \text{ and } B_{L,3} \cong \frac{r}{4\tau_2}\left(\frac{r-k+1}{r-k}\right)$$

For a nominal receiver setting, $r = 2$ (critical damping) and $k = \dfrac{1}{3}$, the loop bandwidth setting constraint becomes:

Second order loop:
$$B_{L,2} = \sqrt{\frac{2\pi}{\phi_{ss,2}}\frac{1}{r}\left(\frac{r+1}{4}\right)^2\left(\frac{df}{dt} + \int_o^T \frac{d^2f}{dt^2}dt\right)} = \sqrt{\frac{9\pi}{16\phi_{ss,2}}\left(\frac{df}{dt} + \int_o^T \frac{d^2f}{dt^2}dt\right)} \tag{3a}$$

Third order loop:
$$B_{L,3} = \sqrt[3]{\frac{2\pi}{\phi_{ss,3}}\frac{1}{rk}\left(\frac{r}{4B_{L,3}}\left(\frac{r-k+1}{r-k}\right)\right)^3\frac{d^2f}{dt^2}} = \sqrt[3]{\frac{\pi}{\phi_{ss,3}}\frac{192}{125}\frac{d^2f}{dt^2}} \tag{3b}$$

Note that aside from the carrier tracking loop, there are also subcarrier and symbol loops in the receivers. However, these loops operate at a much lower frequency compared to the carrier. For the Galileo mission, the subcarrier frequency is 22.5 kHz and the maximum symbol rate is 640 sym/s. They are about five and seven orders of magnitude, respectively, lower than the S-band carrier frequency (2.3 GHz). The effect of Doppler error on these two loops is that much smaller and is therefore not an issue.

3. Thermal noise consideration

The loop signal-to-noise ratio (SNR), ρ, for carrier tracking is defined as [7]:

$$\rho = \frac{P_s}{N_o B_L}L$$

where $\dfrac{P_s}{N_o}$ is available signal-to-noise ratio in 1-Hz bandwidth,

L is the squaring loss in the tracking loop

$$L = \frac{1}{1+2\dfrac{E_s}{N_o}} \text{ for suppressed carrier tracking; } \frac{E_s}{N_o} \text{ being symbol SNR.}$$

$$L = 1 \quad \text{for residual carrier tracking}$$

Normal mode of operations for Galileo tracking is with the suppressed carrier to maximize the data SNR. A minimum operating loop SNR, ρ, of 17 dB is recommended by [7]. Note that the residual carrier tracking can be sustained with a lower threshold of 10 dB. Thus, the maximum allowable bandwidth for a given $\dfrac{P_s}{N_o}$ is:

$$B_L = \frac{P_s}{N_o}\frac{1}{\rho} = 0.02 \frac{P_s}{N_o}L \tag{4}$$

From a thermal consideration, the concern is only placed on carrier tracking loop, not the subcarrier and symbol loops. Because of their lower frequency, the subcarrier and symbol frequencies can be tracked with a much smaller bandwidth, typically in the 30 mHz range. There is sufficient loop SNR to allow for bandwidth widening should it be necessary, though there is not such a need because, as discussed before, the effect of Doppler dynamics are also much less.

4. Optimal bandwidth setting

The optimal bandwidth is the one that satisfies the minimum constraint of (3a), (3b) and the maximum constraint of (4).

Second order loop:
$$\sqrt{\frac{9\pi}{16\phi_{ss,2}}\left(\frac{df}{dt}+\int_o^T\frac{d^2f}{dt^2}dt\right)} \le B_{L,2} \le 0.02\frac{P_s}{N_o}L \tag{5a}$$

Third order loop:
$$\sqrt[3]{\frac{192\pi}{125\phi_{ss,3}}\frac{d^2f}{dt^2}} \le B_{L,3} \le 0.02\frac{P_s}{N_o}L \tag{5b}$$

It should be reminded that the above inequality is derived with an assumption of critical damping (r=2; k=1/3 for third order loop) and a 17-dB loop SNR threshold for suppressed carrier tracking. Different design and operation parameters would have resulted in a different expression.

Note that the five parameters affecting the choice of bandwidth B_L are: received signal SNR $\frac{P_s}{N_o}$, trajectory dynamics $\frac{df}{dt}$ and $\frac{d^2f}{dt^2}$, tracking loop threshold, squaring loss L and allowable phase error ϕ_{ss}. The first and second parameters are largely dictated by the mission design and the accuracy of the modeling. The last three parameters, and to some extent even the second parameter, allow some flexibility. For instance,

1. Trajectory dynamic errors would be smaller for missions operating at S-band, instead of X-band. Because the Doppler is proportional to the carrier frequency, an S-band signal can enjoy a 3.5 reduction in Doppler errors.

2. The threshold required for residual carrier tracking is lower than that of suppressed carrier tracking. The difference can be up to 7 dB, or a factor of 5. The residual carrier modulation, however, would draw some power away from telemetry data.

3. A lower data rate would result in smaller squaring loss since the loss is inversely proportional to the symbol SNR, $\frac{E_s}{N_o}$.

4. A larger allowable phase error, ϕ_{ss}, would allow for more dynamic accommodation. The cost, however, is a degraded performance in the carrier tracking. Since the Galileo mission typically operates with only 0.3 dB link margin, the tracking degradation needs to remain within that limit. A phase error of $\pi/18$ radians (10 degrees), corresponding to a 0.1 dB degradation, is normally targeted.

5. Transient behavior

Before reaching the steady state, the loop response goes through a transient period. Reference [8] identifies the transient error in response to a Doppler rate error for the second order loop as:

$$\phi_2(t) = \frac{\left(\frac{df}{dt}\right)}{\omega_n^2} + \frac{\left(\frac{df}{dt}\right)}{\omega_n^2}\left[\cos\left(\sqrt{1-\zeta^2}\,\omega_n t\right)+\frac{\zeta}{\sqrt{1-\zeta^2}}\sin\left(\sqrt{1-\zeta^2}\,\omega_n t\right)\right]e^{-\zeta\omega_n t}$$

where ζ is the damping factor and ω_n is the natural frequency of the loop.

The above equation applies to an under-damping ($\zeta < 1$) condition. For critical damping ($\zeta = 0.707$, or equivalently $r = 2$), the maximum oscillation is only 5% above the steady state error. Due to the exponential term, the settling time of the transient behavior is also short, in the order of $\frac{5}{\zeta\omega_n}$ seconds. With the loop bandwidth being a fraction of a Hz, the transient period normally only lasts about 10 seconds. Because the difference between steady state and transient responses is small, both in term of magnitude and time scale, the simpler steady state approach is valid.

III. DATA ANALYSIS

Table 1 lists selected encounters with Jovian satellites by the Galileo spacecraft [9, 10]. These encounters are selected among all available because of their expected high Doppler dynamics. They span across the prime mission, which ended in January 1998, and the two extended missions thereafter. These encounters enable a close-up study of the satellite surface and its environment. The four largest moons of Jupiter - Io, Europa, Ganymede and Callisto - are the focus of study. The name of the encounter activity, e.g, C3, is comprised of the moon under study and its orbital sequence.

Table 1: Doppler and SNR conditions of selected encounters

Encounter	Time of Closest Approach	Altitude, km	Max. Doppler Error, Hz	Max. Doppler Rate Error, Hz/s	Max. Acceleration Error, Hz/s²	Signal level (Ps/No), dB
G1	6/27/96 07:04	844	36	0.09	0.00045	19.4 (17.2)
G2	9/6/96 19:37	250	26	0.06	0.0004	16.2 (15)
C3	11/4/96 14:20	1104	42	0.07	0.0003	15.1 (15)
E6	2/20/97 17:54	587	15	0.042	0.00092	17 (15.4)
C9	6/25/97 14:24	416	1.4	0.003	0.000012	17.7 (17.5)
C10	9/17/97 00:54	524	8	0.02	0.00016	15.5 (15)
I24	10/11/99 05:06	2520	3.2	0.01	0.00034	19.5 (18)
I25	11/26/99 04:40	2120	8.4	0.028	0.00093	17 (15)
C30	5/25/01 12:14	123	2.2	0.03	0.00029	

The spacecraft altitude at the time of closest approach is given in the third column. Compared to a previous flyby made by Voyager 1 and 2 spacecraft, some of these approaches are a few hundred times closer. As a result, the impact on Doppler is quite pronounced. The maximum uncertainty of Doppler offset, Doppler rate and Doppler acceleration are given in the fourth, fifth and sixth columns. Of these encounters, all except C9 and C30 are under 2-way tracking. The 2-way errors are more pronounced compared with 1-way tracking.

Note that the acceleration error ranges from 0.5% to 3% of Doppler rate error. Assuming a 1% error level and a linear acceleration profile, the integral term in (5a) indicates that the phase error from the acceleration would be about the same as that from the Doppler rate for any perturbation over 200 seconds. In most Galileo encounters, the trajectory perturbation lasts up to 700 seconds. Thus, the effect of Doppler acceleration error on the second order loop is significant and cannot be neglected.

The last column shows the available signal-to-noise ratio at the time of closest approach. The second value in the parentheses refers to the SNR at the beginning of the track. Its lower value reflects the higher system noise temperature at low elevation. The difference, as in the G1 encounter, can be as large as 2.2 dB (66%). One can take advantage of the available SNR by using a smaller bandwidth at the start of track and widen it at the time of encounter. Although the receivers are designed to support such a change in bandwidth in mid track, Galileo operations tends to stay with single bandwidth because of the concern on operational complexity.

For normal tracking outside of the encounter period, the bandwidth for the second order loop is nominally set at 0.3 Hz. For the third order loop, 0.25 Hz is used. For the encounters, the bandwidth is widened, typically to 0.5 +/- 0.1 Hz.

Often there is not enough SNR to afford the wide bandwidth required for Doppler dynamics. As a result, certain data outage is expected. The mission design team guards against such data outage by using filled data. The result of the encounters is presented in Table 2 [11].

Table 2: Results from selected Galileo encounters

Encounter	Time of closest approach	Outage, 2nd order loop	Outage, 3rd order loop
G1	07:04	06:59:24 – 07:05:35	none
G2	19:37	19:34:33 - 19:37:34	none
C3	14:20	14:12:54 - 14:39:19	14:45:47 – 14:55:53
E6	17:56	n/a due to occultation	n/a due to occultation
C9	14:24	n/a due to occultation	n/a due to occultation
C10	00:54	00:46:06 – 00:52:55*	none
I24	05:06	04:45:52 – 04:56:53	04:45:36 – 04:57:10
I25	04:40	04:32:04 – 04:35:51	04:41:20 – 04:41:45
C30	12:14	n/a due to occultation	n/a due to occultation

* Encounter occurred over period of hand-over between Madrid and Goldstone tracking complex. Loss of lock is seen at Madrid, but not at Goldstone.

Although the data is limited, a few observations can be drawn:

(1) Occultation occurs quite often. During the occultation, the signal is blocked by Jupiter's moon. These events are dedicated to radio science study of the planetary atmosphere. During radio science investigation, change in the phase of the signal carrier is used to infer the characteristics of the medium through which the signal traverses. Telemetry data are normally turned off to maximize the carrier power. These operating conditions hamper this study effort in two ways. First, the perturbation profile is changed. No longer does the signal appear throughout the entire perturbation. Rather, it disappears at the closest approach or shows up near the period of maximum Doppler from its occultation egress. A signal re-acquisition becomes necessary. The process of reacquiring removes all perturbation up to that point. As a result, dynamic conditions become smaller. Secondly, with the presence of the carrier, the phase lock loop can be operated in the residual carrier mode. As mentioned in section II.3, residual carrier tracking requires a lower threshold than suppressed carrier tracking. Therefore, the bandwidth can be widened and tracking problems are eased.

(2) A period of data outage does not always coincide with maximum Doppler conditions. As seen in the I24 and I25 encounters, the receiver can lose lock prior to the closest approach and quickly recover. The new acquisition allows it to maintain lock during the closest approach.

(3) The third order loop can produce a better performance than the second order loop, as seen with the G2 and I25 encounters. There are, however, opposing data. For example, during the I24 encounter, both loops are briefly out of lock but the outage of the third order loop is longer than that of the second order loop. Also, for the C3 encounter, the third order loop, while managing to track through the closest approach, stumbles out of lock 25 minutes later.

(4) While the existing data support the behavioral predictions, unfortunately, no definitive conclusion can be drawn regarding how well the PLL mathematical model applies to spacecraft tracking. One reason being that there is

not enough data to warrant a precise characterization. The other being that a recent re-examination of trajectory predictions casts a doubt on the accuracy of the estimated Doppler rate and acceleration errors for all encounters except C30. It is believed that the previous figures are underestimated. Recalculated figures however are not available for this study.

IV. CONCLUSION

This paper has presented a consideration for receiver bandwidth setting that would satisfy both thermal and dynamic constraints. Thermal noise viewpoint favors a narrow bandwidth. In contrast, the need to accommodate high dynamic uncertainty at planetary encounters pushes for wider bandwidth. A review of mathematical formulation leading to the bandwidth setting is provided. The analysis is given for both second order and third order loops.

For the second order loop, both frequency error and acceleration error affect the receiver performance. Trajectory analysis from Galileo mission suggests that the effect of the Doppler acceleration error is quite significant. A third order loop can help to remove this particular effect. Data obtained from different Galileo encounters tend to support this conclusion. The results are also consistent with overall predicted supportability; however, the data set is limited and does not allow for a good characterization on the model accuracy.

Some operational considerations that can help to alleviate the problem are identified. A lower operating frequency, e.g. S-band instead of X-band, would render less dynamics. The use of residual, instead of suppressed, carrier modulation would reduce the required tracking threshold. An increase in the link margin, by reducing the data rate, would tolerate a larger phase error. Finally, a practice of having bandwidth changed to take advantage of higher SNR available in mid track would better accommodate the dynamics.

ACKNOWLEDGMENT

REFERENCES

[1] Galileo Mission Homepage, www.galileo.jpl.nasa.gov.
[2] F. M. Gardner, *Phaselock Techniques*, 2rd ed., John Wiley & Sons, 1979.
[3] R.J. Haw, "Doppler frequency, frequency rate, and frequency acceleration uncertainties for the I25 encounter", Jet Propulsion Laboratory, unpublished.
[4] R.C. Tausworth, *Theory and Practical Design of Phase-Locked Receivers*, JPL Technical Report No. 32-819, Jet Propulsion Laboratory, California, February 1966.
[5] J. K. Holmes, *Coherent Spread Spectrum Systems*, John Wiley & Sons Inc., New York, 1982.
[6] S. Aguierro, W.J.Hurd, "Design and Performance of Sampled Data Loops for Subcarrier and Carrier Tracking", TDA Progress Report 42-79, Jet Propulsion Laboratory, California, October 1984.
[7] *810-005, DSMS Telecommunications Link Design Handbook*, D-19379, Rev. E, Jet Propulsion Laboratory, California, January 2001
[8] L.A. Hoffman, "Receiver Design and the Phase-Lock Loop", Aerospace Corporation, El Segundo, CA, May 1963
[9] J.L. Bell, J.R. Johannesen, "Plots of Earth-line Velocity and Acceleration for Perturbed Encounters for the 960110 Tour", GLL-NAV-96-19, April 9, 1996, Jet Propulsion Laboratory, unpublished.
[10] W. Kirkhofer, P. Antreasian, T. McElrath, R.J. Haw, "Doppler frequency, frequency rate, and frequency acceleration uncertainties for [various] encounters", Jet Propulsion Laboratory, unpublished.
[11] Operational records from the Galileo Telecom Operations Engineering team, Jet Propulsion Laboratory, unpublished.